Available online at www.sciencedirect.com

ScienceDirect

Ceramics International 40 (2014) 2857–2861

CERAMICS INTERNATIONAL

www.elsevier.com/locate/ceramint

Corrosion protection by zirconia-based thin films deposited by a sol–gel spin coating method

Mohsen Norouzi[a,*], Abbas Afrasiabi Garekani[a,b]

[a]Department of Materials Engineering, Corrosion and Protection of Materials, Khorasan Razavi, Neyshabur, Science and Research Branch, Islamic Azad University, Neyshabur, Iran

[b]Research Institute of Food Science and Technology, Mashhad, Iran

Received 1 September 2013; received in revised form 3 October 2013; accepted 6 October 2013
Available online 11 October 2013

Abstract

This paper focuses on the structure and corrosion behavior of 316L stainless steel coated by inorganic ZrO_2, hybrid ZrO_2–PMMA, and combined inorganic–hybrid films. The coatings were deposited by a particulate sol–gel spin-coating route, using carboxymethyl cellulose as a nanoparticle dispersant. The electrochemical evaluations were conducted in a simulated body fluid, via potentiodynamic polarization and impedance spectroscopic experiments. According to the results, the hybrid coating presented a better corrosion protection compared to the inorganic coating, due to a lesser density of structural defects. However, the best corrosion resistance was found for a combined coating which consists of an inorganic bottom layer and a hybrid top layer, due to a desirable compromise of good adhesion and low defect density.

Keywords: A. Sol–gel processes; B. Surfaces; C. Corrosion; D. ZrO_2

1. Introduction

Metals and alloys are the oldest materials used in surgical purposes to make devices for fracture fixation, joint replacement, external splints, braces, traction apparatus, and dental amalgams [1]. Nowadays, the widely used metallic biomaterials include stainless steels, titanium and its alloys, and cobalt–chromium-based alloys, as well as tantalum, niobium, and gold. Stainless steels, typically AISI 316L, are conventionally used in orthopedics, with the main advantages of low cost, good mechanical properties, sufficient corrosion resistance, and easy processing. However, problems have been found with this type of medical-grade stainless steels. The most important problem is the negative effect of metal ions or fretting debris released from the implant due to corrosion and wear [2,3].

In the biomaterials field, as well as the modification of chemical composition, surface modification techniques are used with the principal purpose of an improvement in corrosion resistance, wear resistance, antibacterial property, and tissue compatibility [1,4]. Coating, as one of these methods, not only can increase the corrosion resistance of the implant, but also can improve the implant–tissue interaction. Among various methods used to process coatings, the sol–gel deposition process has advantages, such as high homogeneity, low sintering temperatures, and simplicity of complex shape coating [5,6].

Zirconia (ZrO_2) is one of the most interesting ceramics in biomedical purposes, due to biocompatibility and bioactivity. In the literature, there are a number of studies on the corrosion protection of stainless steels by zirconia-based coatings prepared by polymeric sol–gel processes, especially in acidic electrolytes, via polarization experiments [7–10]. It has been known that ZrO_2 has a high expansion coefficient very close to those of stainless steels, which can reduce the formation of cracks during high-temperature curing processes. ZrO_2 presents also a good chemical stability and high hardness, making it a good protective material [11]. However, to our knowledge, little systematic work has been reported on the corrosion protection of 316L stainless steel in a simulated body fluid by zirconia-based thin films processed by particulate sol–gel methods, rather than polymeric sol–gel processes.

In this paper, three types of coating, inorganic ZrO_2, hybrid ZrO_2–PMMA, and combined inorganic-–hybrid films, were deposited on 316L stainless steel, via a particulate sol–gel spin

*Corresponding author. Tel.: +98 918 860 8209.
E-mail address: Mohsen_norouzi74@yahoo.com (M. Norouzi).

0272-8842/$ - see front matter © 2013 Elsevier Ltd and Techna Group S.r.l. All rights reserved.
http://dx.doi.org/10.1016/j.ceramint.2013.10.027

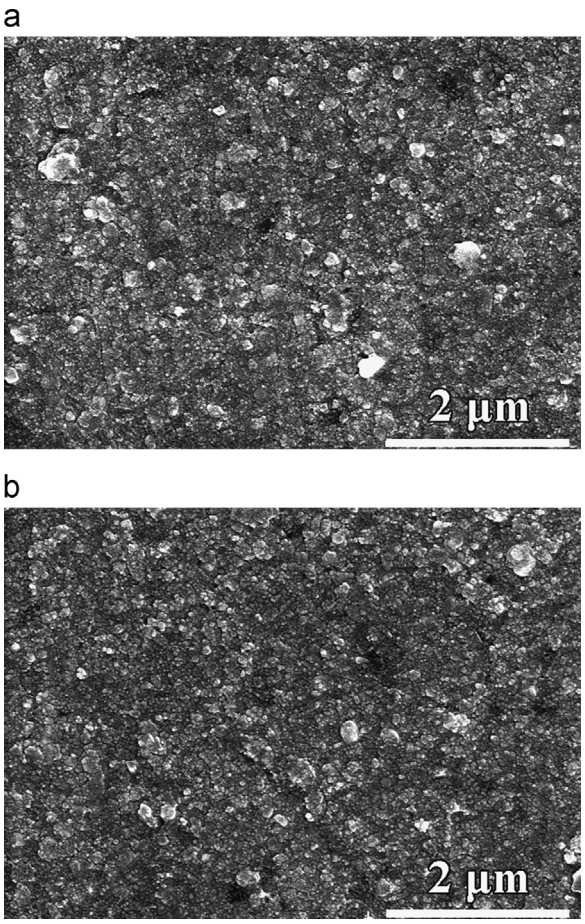

Fig. 1. Morphological SEM micrograph of the inorganic (a) and hybrid (b) coatings.

coating method. After studying the coating structure, the corrosion behavior of the specimens was also evaluated in a simulated body fluid, via potentiodynamic polarization and electrochemical impedance spectroscopic experiments.

2. Materials and methods

316L austenitic stainless steel discs were ground by emery papers, polished by alumina powders, and ultrasonically cleaned in acetone, ethanol, and distilled water. Three types of sol–gel derived coatings were deposited on the substrate: inorganic ZrO_2, hybrid ZrO_2–PMMA, and a combination of the inorganic and hybrid coatings. To process the inorganic coating, $ZrCl_4$ (Alfa Aesar, 99.5%) was first dissolved in deionized water. Then, by the dropwise addition of a NaOH solution, the pH of the solution was increased to 7 (hydrogel). To remove chloride ions, the hydrogel was repeatedly rinsed with deionized water. Afterwards, 75 mL of deionized water and 2 wt% carboxymethyl cellulose (CMC, sodium salt, Alfa Aesar) as a dispersing agent were added to the product. To prepare the hybrid $ZrO_2$10 vol% PMMA coating, appropriate amount of polymethyl methacrylate (PMMA, Alfa Aesar) dissolved in acetone was added to the prepared sol. The sols were separately spin-coated on the substrate at a

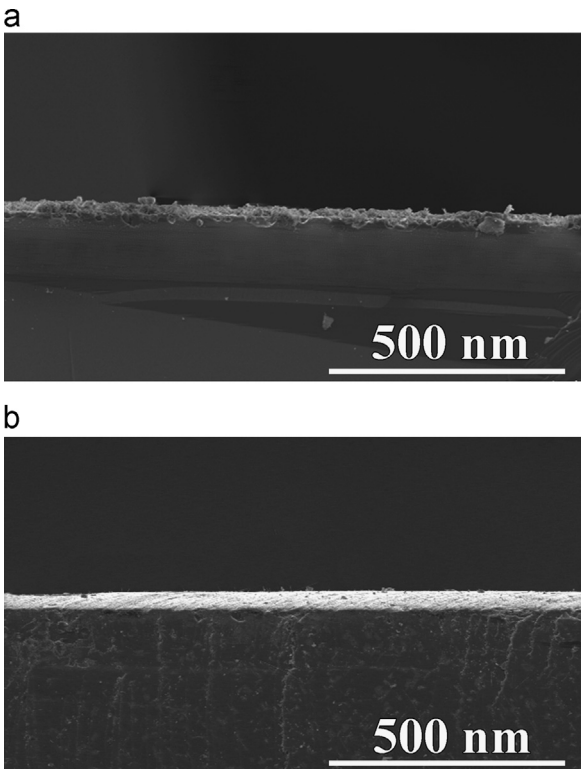

Fig. 2. Cross sectional SEM micrograph of the inorganic (a) and hybrid (b) coatings.

speed of 3000 rpm. Finally, the inorganic and hybrid coatings were sintered at 900 °C and 150 °C for 1 h, respectively. The combined coating also consisted of an inorganic bottom layer and a hybrid top layer, and was electrochemically compared with the double-layer inorganic and hybrid coatings.

The sample surfaces were studied using a scanning electron microscope (SEM, Leica Cambridge) and atomic force microscope (AFM, Bruker AXS). The film adhesion to the substrate was also evaluated by the adhesive tape test, in accordance with ASTM D 3359. The electrochemical corrosion behavior was investigated in the simulated body fluid (SBF) [12] at a pH value of 7.4. A platinum wire and saturated calomel electrode (SCE) were employed as the auxiliary and reference electrodes, respectively. The samples were firstly immersed in SBF for 1 h to obtain a steady-state open circuit potential (*ocp*). Subsequently, anodic potentiodynamic polarization curves were obtained at a scan rate of 1 mV s^{-1} from −0.1 V vs. *ocp* to the transpassive potential. Electrochemical impedance spectroscopic measurements were also performed over 10 frequency decades from 5 kHz to 10 mHz with an excitation potential amplitude of 10 mV at the *ocp*.

3. Results and discussion

Fig. 1 depicts a top-view SEM micrograph of the coatings modified with the CMC addition, showing high-coverage, uniform, and crack-free coatings. The desirable characteristics of the films are attributed to the presence of CMC in the sol [13–15]. The cross-sectional SEM image of the coated samples

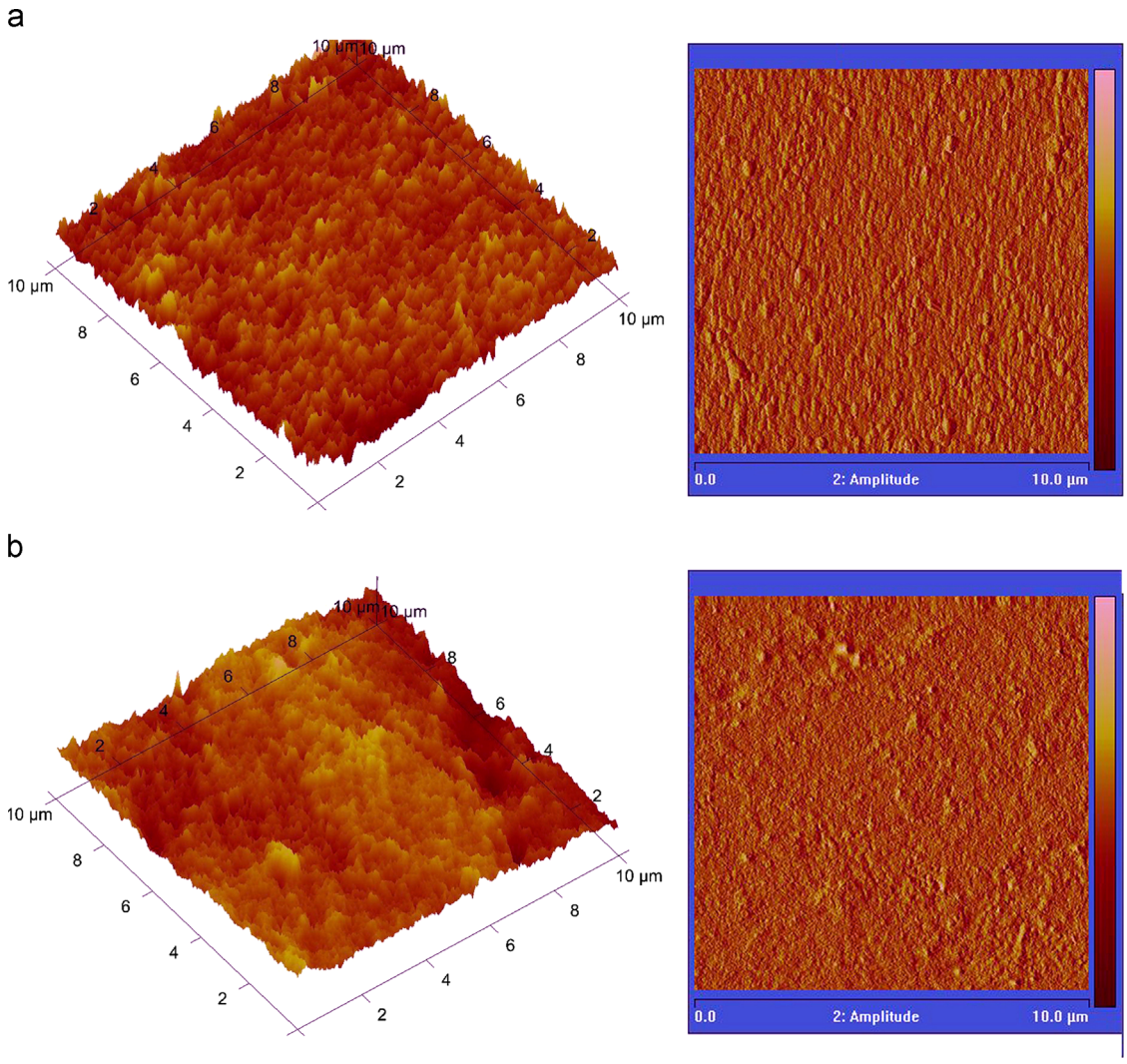

Fig. 3. Two and three dimensional AFM images of the inorganic (a) and hybrid (b) coatings.

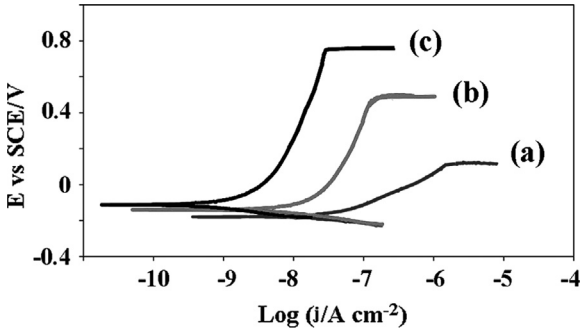

Fig. 4. Potentiodynamic polarization curves for the substrate uncoated (a) and coated with the monolayer inorganic (b) and hybrid (c) coatings.

is also shown in Fig. 2. As can be seen, the film has uniformly covered the substrate and a good adhesion to the substrate has been obtained. In addition, the film thickness is estimated to be about 60 nm for both of the coatings. Fig. 3 indicates two and three dimensional AFM images of the inorganic and hybrid films, suggesting smooth, uniform, and dense coatings, as confirmed by SEM. The average roughness value of the inorganic and hybrid films over areas of $10 \times 10\ \mu m^2$ is 20 and 12 nm, respectively. The slightly higher roughness value of the inorganic film, compared with the hybrid film, is due to the higher firing temperature used and thereby nanoparticle growth.

Fig. 4 presents the polarization curve of the samples uncoated and coated with the inorganic ZrO_2 and hybrid ZrO_2–PMMA thin films. The electrochemical data are listed in Table 1. That is, the anti-corrosion behavior is improved in this order: substrate < ZrO_2 < ZrO_2–PMMA, where the coatings

Table 1
Corrosion potential (E_{corr}), corrosion current density (j_{corr}), passive current density (j_p), and breakdown potential (E_b), extracted from Fig. 4, in which the coatings are monolayers.

Sample	E_{corr} vs. S CE /(mV)	j_{corr} (A/cm^2)	j_p (A/cm^2)	E_b vs. SCE /(mV)
Substrate	−210	5.6×10^{-8}	7.2×10^{-7}	70
Inorganic coated	−145	6.2×10^{-9}	6.3×10^{-8}	410
Hybrid coated	−110	1.2×10^{-9}	1.1×10^{-8}	720

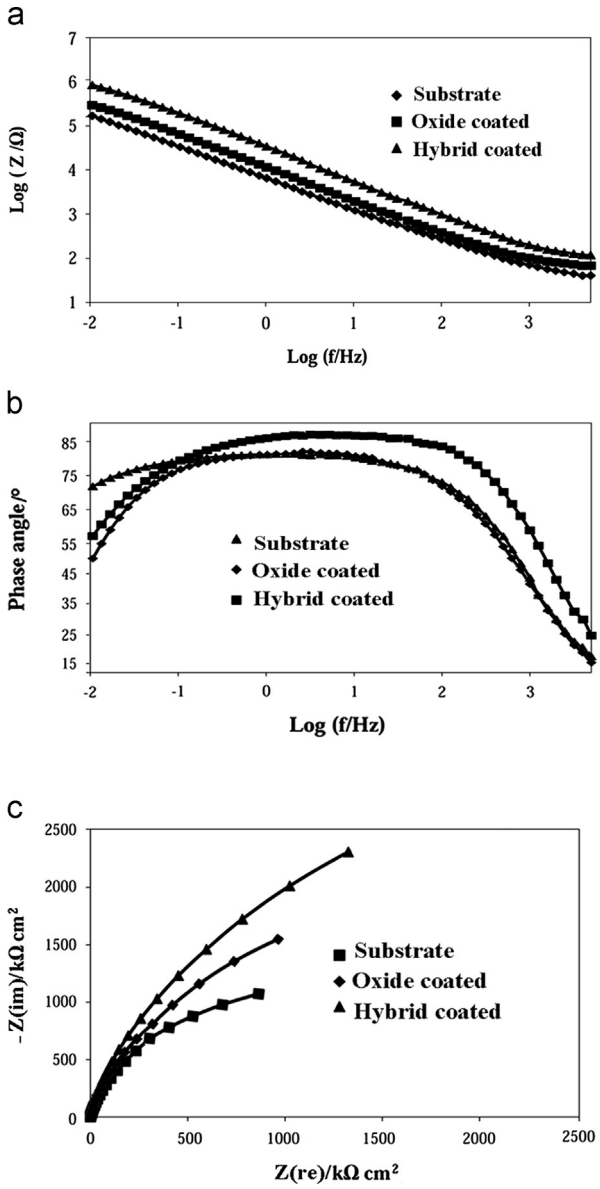

Fig. 5. Bode impedance (a), Bode phase angle (b), and Nyquist (c) plots for the uncoated and coated samples.

act as a physical protective barrier for blocking the electrochemical processes. The Nyquist and Bode impedance plots of the samples are shown in Fig. 5. According to the impedance plots, the value of impedance increases in this order: substrate < ZrO_2 < ZrO_2–PMMA. It means that the hybrid-coated sample exhibits the lowest corrosion rate and the uncoated sample presents the highest susceptibility towards corrosion, as realized by the polarization tests. An equivalent electrical circuit (Fig. 6) was used for the quantitative analyses of the impedance spectra. Note that R_{sol} is the electrolyte resistance, R_{po} is the resistance of film pores, and R_{ct} is the charge transfer resistance. CPE denotes a constant phase element, where $CPE_c(Q_c,n_c)$ and $CPE_{dl}(Q_{dl},n_{dl})$ correspond to the geometric capacitance of the film and double layer, respectively. The equivalent electrical circuit parameters are listed in Table 2. Based on polarization resistance (R_p), the corrosion

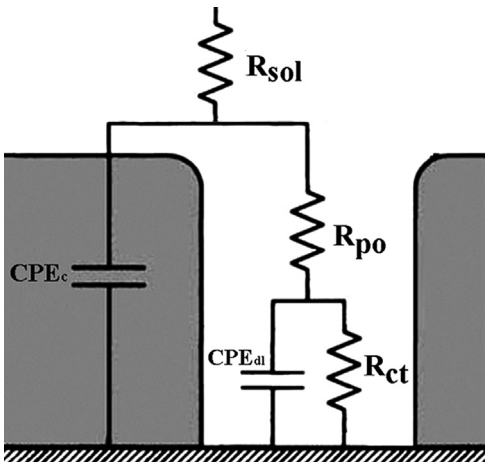

Fig. 6. Equivalent electrical circuit used to model the impedance data [19].

rate shows an increasing trend in this order: ZrO_2–PMMA < ZrO_2 < substrate.

The higher corrosion protection of the hybrid coating compared with the inorganic coating is due to its lower defect density. Sol–gel coatings can corrode only through their defects which allow the electrolyte access to the metal surface [16]. PMMA fills an amount of porosities and makes the coating denser. On the other hand, PMMA makes the hybrid thin film more hydrophobic, compared with the inorganic coating, which impedes the electrolyte access to the metal/coating interface [17–19].

Fig. 7 presents the polarization curve of the double-layer inorganic, hybrid, and combined coated samples. According to the electrochemical data listed in Table 3, the corrosion protection of the substrate by the coatings increases in the order: inorganic < hybrid < combined. The inferior corrosion resistance of the sample coated with the pure inorganic film is due to the absence of PMMA and the highly porous nature of the coating [18,19]. To find the reason of the corrosion protection improved by the combined coating, the film adhesion to the substrate was considered. Based on the adhesive tape test, the adhesion of the combined coating, like the inorganic coating, is rated as 5B (i.e. a desirable adhesion). The formation of a covalent bond between the bottom layer and the substrate is the source of the good adhesion. But the adhesion of the hybrid coating is rated as 4B, i.e. a weaker adhesion compared with 5B. This is because of the low-temperature sintering process used, where the efficient covalent bonds are fewer. Thus, it is inferred that the better adhesion of the combined coating is the source of the higher corrosion resistance of the specimen coated with this film [18].

Comparing Fig. 4 with Fig. 7 and Table 1 with Table 3, it is also realized that the double-layer coatings present a better corrosion protection than the monolayer ones, as expected because the film thickness increases and the electrolyte access to the substrate is retarded. Finally, it is concluded that the sol–gel deposition route used in this work is an effective approach to improving the corrosion resistance of the austenitic stainless steels.

Table 2
Equivalent electrical circuit parameters obtained by the impedance studies.

Sample	R_{po} (Ω cm^2)	Q_c ($\mu\Omega^{-1}$ sn_c cm^{-2})	n_c	R_{ct} (MΩ cm^2)	Q_{dl} ($\mu\Omega^{-1}$ sn_{dl} cm^{-2})	n_{dl}
Substrate	60.0 ± 12.2	2.8 ± 0.3	0.88	1.5 ± 0.3	10.4 ± 1.1	0.99
Inorganic coated	119.8 ± 10.5	2.9 ± 0.2	0.92	2.3 ± 0.1	5.3 ± 0.4	0.90
Hybrid coated	211.2 ± 17.0	1.6 ± 0.5	0.98	3.5 ± 0.2	2.0 ± 0.5	0.87

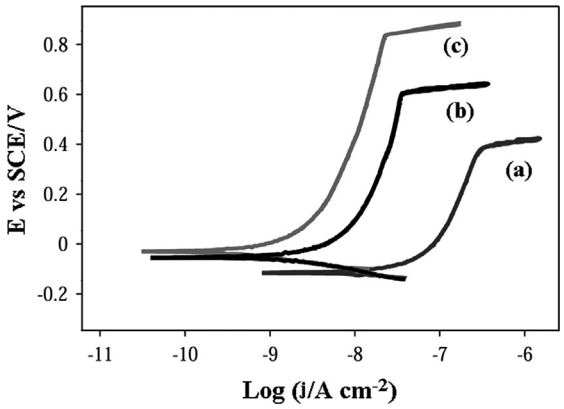

Fig. 7. Potentiodynamic polarization curves for the substrate coated with the double-layer inorganic (a), hybrid (b), and combined (c) coatings.

Table 3
Electrochemical data extracted from Fig. 7, in which the coatings are double-layers.

Sample	E_{corr} vs. SCE /(mV)	j_{corr} (A/cm^2)	j_p (A/cm^2)	E_b vs. SCE /(mV)
Inorganic coating	−140	5.46×10^{-9}	6.12×10^{-8}	440
Hybrid coating	−110	1.15×10^{-9}	1.01×10^{-8}	735
Combined coating	−60	0.97×10^{-9}	0.95×10^{-8}	795

4. Conclusions

In this paper, the structure and corrosion behavior of 316L stainless steel coated by ZrO_2, ZrO_2–PMMA, and combined films were studied. The following conclusions can be drawn from this work:

1. Zirconia-based, sol–gel derived, thin films were successfully processed, where the thickness of each layer was found to be about 60 nm;
2. the prepared coatings improved the corrosion resistance of the substrate, in terms of corrosion potential, corrosion current density, passivity, and passive potential range;
3. the corrosion protection by the ZrO_2–PMMA hybrid coating was better than the inorganic ZrO_2 coating.
4. the combined coating which consisted of the ZrO_2 bottom layer and the ZrO_2–PMMA top layer presented the best corrosion protection.

References

[1] U.K. Mudali, T.M. Sridhar, B. Raj, Corrosion of bio implants, Sadhana 28 (2003) 601–637.
[2] K. Yang, Y. Ren, Nickel-free austenitic stainless steels for medical applications, Sci. Technol. Adv. Mater. 11 (2010) 1–13.
[3] M. Sumita, T. Hanawa, S.H. Teoh, Development of nitrogen-containing nickel-free austenitic stainless, Mater. Sci. Eng. C 24 (2004) 753–760.
[4] J.Anusavice Kenneth, Philips Science of Dental Materials, 11th ed., Saunders Elsevier, St Louis, 2005.
[5] C.J. Brinker, A.J. Hurd, P.R. Shunrk, Review of sol–gel thin film formation, J. Non-Cryst. Solids 147 (1992) 424–436.
[6] J.D. Wright, N.A.J. Sommerdijk, Sol–Gel Materials Chemistry and Applications, CRC Press, OPA Overseas Publishers Association (Taylor & Francis Group), 2001.
[7] F. Perdomo, P.D. Lima, M.A. Aegerter, L.A. Avaca, Sol–gel deposition of ZrO_2 films in air and in oxygen-free atmospheres for chemical protection of 304 stainless steel: a comparative corrosion study, J. Sol–Gel Sci. Technol. 15 (1999) 87–91.
[8] M. Atik, F.P. Luna, S.H. Messaddeq, M.A. Aegerter, Ormocer (ZrO_2–PMMA) films for stainless steel corrosion protection, J. Sol–Gel Sci. Technol. 8 (1997) 517–522.
[9] S.H. Messaddeq, S.H. Pulcinelli, C.V. Santilli, A.C. Guastaldi, Y. Messaddeq, Microstructure and corrosion resistance of inorganic–organic (ZrO_2–PMMA) hybrid coating on stainless steel, J. Non-Cryst. Solids 247 (1999) 164–170.
[10] E. Nouri, M. Shahmiri, H.R. Rezaie, F. Talayian, Investigation of structural evolution and electrochemical behaviour of zirconia thin films on the 316L stainless steel substrate formed via sol–gel process, Surf. Coat. Technol 205 (2011) 5109–5115.
[11] D. Wang, G.P. Bierwagen, Sol–gel coatings on metals for corrosion protection, Prog. Org. Coat 64 (2009) 327–338.
[12] T. Kokubo, H. Takadama, How useful is SBF in predicting in vivo bone bioactivity?, Biomaterials 27 (2006) 2907–2915
[13] S. Song, A. Lopez-Valdivieso, C. Martinez-Martinez, R. Torres-Armenta, Improving fluorite flotation from ores by dispersion processing, Miner. Eng. 19 (2006) 912–917.
[14] E. Salahinejad, M.J. Hadianfard, D.D. Macdonald, M. Mozafari, D. Vashaee, L. Tayebi, Zirconium titanate thin film prepared by an aqueous particulate sol–gel spin coating process using carboxymethyl cellulose as dispersant, Mater. Lett. 88 (2012) 5–8.
[15] E. Salahinejad, M.J. Hadianfard, D.D. Macdonald, M. Mozafari, D. Vashaee, L. Tayebi, Multilayer zirconium titanate thin films prepared by a sol–gel deposition method, Ceram. Int. 39 (2013) 1271–1276.
[16] E. Setare, K. Raeissi, M.A. Golozar, M.H. Fathi, The structure and corrosion barrier performance of nanocrystalline zirconia electrodeposited coating, Corros. Sci. 51 (2009) 1802–1808.
[17] J. Gallardo, A. Duran, J.J. de Damborenea, Electrochemical and in vitro behaviour of sol–gel coated 316L stainless steel, Corros. Sci 46 (2004) 795–806.
[18] E. Salahinejad, M.J. Hadianfard, D.D. Macdonald, M. Mozafari, D. Vashaee, L. Tayebi, A new double-layer sol–gel coating to improve the corrosion resistance of a medical-grade stainless steel in a simulated body fluid, Mater. Lett. 97 (2013) 162–165.
[19] E. Salahinejad, M.J. Hadianfard, D.D. Macdonald, S. Sharifi-Asl, M. Mozafari, K.J. Walker, A. Tahmasbi Rad, S.V. Madihally, D. Vashaee, L. Tayebi, Surface modification of stainless steel orthopedic implants by sol–gel $ZrTiO_4$ and $ZrTiO_4$-PMMA coatings, J. Biomed. Nanotechnol. 9 (2013) 1327–1335.